432x432 SW/MW FPAs with Extended Dynamic Range

P.H. Zimmermann, A. Hairston, T. Parodos, P. Norton, R. Hines, J. Welsch
and B. Yeadon
Lockheed Martin IR Imaging Systems
Lexington, Massachusetts 02173

ABSTRACT

This is the first report on results for Lockheed Martin's radiation-hardened 432x432 MW HgCdTe Focal Plane Arrays (FPAs) with extended dynamic range. The extended dynamic range concept has also been successfully implemented in a 768 x 6 TDI scanning FPA. These large format FPAs are designed for space surveillance applications. The instantaneous dynamic range of the staring FPAs is up to 118dB. Excellent operability and uniformity has been measured. Near BLIP NEI has been demonstrated for SW (3.6 µm cutoff) detectors operating at 120K at 1.8E12 ph/cm^2-s background irradiance and MW (4.8 µm cutoff) detectors operating at 120K at 8.0E12 ph/cm^2-s background irradiance. These FPAs utilize the Lockheed Martin Federal Systems (LMFS) 0.8 µm radiation-hardened CMOS process with two layer polysilicon and depletion mode capacitor options for total dose radiation hardness.

In this paper we describe the results achieved with our new 432x432 FPAs and also our new 768 x 6 scanning FPAs. The detectors were fabricated using our production LPE material growth process and a multi-layer anti-reflection coating to give high and uniform quantum efficiency of 90% over the large active areas. The responsivity standard deviation is only 2.4% of the average responsivity. The ROICs have a dual-gain feature that gives a very high maximum instantaneous dynamic range of 118dB. These FPAs have demonstrated a 80% of-BLIP NEI of 3.0E9 ph/cm^2-s at a background of 1.8E12 ph/cm^2-s, an integration time of 18 ms and a cutoff of 3.6 µm at 120K. NEI and response operability have been measured at over 99%. Differential responsivity linearity is typically 0.5%. Data for MW 432x432 also show near BLIP limited performance. The FPA is low power, drawing only 85 mW, even though it has a CTIA amplifier input for each detector to give good performance at low backgrounds.

1.0 INTRODUCTION AND OVERVIEW

The Extended Dynamic Range (EDR) FPA is a large format FPA designed to provide a very large instantaneous dynamic range. In a previous IRIS DSGM paper we reported the first results[1] on our radiation-hardened MW HgCdTe staring FPAs in 256x256 and 400x400 formats at 110K and 120K. This new larger staring FPA array format is 432 x 432. The ROIC has an automatic gain selection feature that selects and reports the transimpedance gain on a pixel by pixel basis. The gain data is transmitted as digital state data in

REPORT DOCUMENTATION PAGE

Form Approved OMB No. 0704-0188

1. REPORT DATE (DD-MM-YYYY)	2. REPORT TYPE	3. DATES COVERED (FROM - TO)
01-01-1998	Conference Proceedings	xx-xx-1998 to xx-xx-1998

4. TITLE AND SUBTITLE
432x432 SW/MW FPAs with Extended Dynamic Range
Unclassified

5a. CONTRACT NUMBER

5b. GRANT NUMBER

5c. PROGRAM ELEMENT NUMBER

6. AUTHOR(S)
Zimmermann, P. H. ;
Hairston, A. ;
Parodos, T. ;
Norton, P. ;
Hines, R. ;

5d. PROJECT NUMBER

5e. TASK NUMBER

5f. WORK UNIT NUMBER

7. PERFORMING ORGANIZATION NAME AND ADDRESS
Lockheed Martin IR Imaging Systems
Lexington, MA02173

8. PERFORMING ORGANIZATION REPORT NUMBER

9. SPONSORING/MONITORING AGENCY NAME AND ADDRESS
Director, CECOM RDEC
Night vision and Electronic Sensors Directorate, Security Team
10221 Burbeck Rd.
Ft. Belvoir, VA22060-5806

10. SPONSOR/MONITOR'S ACRONYM(S)

11. SPONSOR/MONITOR'S REPORT NUMBER(S)

12. DISTRIBUTION/AVAILABILITY STATEMENT
APUBLIC RELEASE
,

13. SUPPLEMENTARY NOTES
See Also ADM201041, 1998 IRIS Proceedings on CD-ROM.

14. ABSTRACT
This is the first report on results for Lockheed Martin?s radiationhardened 432x432 MW HgCdTe Focal Plane Arrays (FPAs) with extended dynamic range. The extended dynamic range concept has also been successfully implemented in a 768 x 6 TDI scanning FPA. These large format FPAs are designed for space surveillance applications. The instantaneous dynamic range of the staring FPAs is up to 118dB. Excellent operability and uniformity has been measured. Near BLIP NEI has been demonstrated for SW (3.6 mm cutoff) detectors operating at 120K at 1.8E12 ph/cm2-s background irradiance and MW (4.8 mm cutoff) detectors operating at 120K at 8.0E12 ph/cm2-s background irradiance. These FPAs utilize the Lockheed Martin Federal Systems (LMFS) 0.8 mm radiationhardened CMOS process with two layer polysilicon and depletion mode capacitor options for total dose radiation hardness. In this paper we describe the results achieved with our new 432x432 FPAs and also our new 768 x 6 scanning FPAs. The detectors were fabricated using our production LPE material growth process and a multilayer anti-reflection coating to give high and uniform quantum efficiency of 90% over the large active areas. The responsivity standard deviation is only 2.4% of the average responsivity. The ROICs have a dual-gain feature that gives a very high maximum instantaneous dynamic range of 118dB. These FPAs have demonstrated a 80% of-BLIP NEI of 3.0E9 ph/cm2-s at a background of 1.8E12 ph/cm2-s, an integration time of 18 ms and a cutoff of 3.6 mm at 120K. NEI and response operability have been measured at over 99%. Differential responsivity linearity is typically 0.5%. Data for MW 432x432 also show near BLIP limited performance. The FPA is low power, drawing only 85 mW, even though it has a CTIA amplifier input for each detector to give good performance at low backgrounds.

15. SUBJECT TERMS

16. SECURITY CLASSIFICATION OF:			17. LIMITATION OF ABSTRACT	18. NUMBER OF PAGES	19. NAME OF RESPONSIBLE PERSON
			Public Release	10	Fenster, Lynn lfenster@dtic.mil
a. REPORT Unclassified	b. ABSTRACT Unclassified	c. THIS PAGE Unclassified			19b. TELEPHONE NUMBER International Area Code Area Code Telephone Number 703767-9007 DSN 427-9007

Standard Form 298 (Rev. 8-98)
Prescribed by ANSI Std Z39.18

parallel with the analog output. It is designed for irradiances from 1E11 to 8E14 ph/cm^2-s, with a performance emphasis on the 1E12 to 1E13 ph/cm^2-s range. Two spectral bands have been fabricated, an SW band with a cutoff of 3.6 μm and an MW band with a cutoff of 4.8 μm. Both bands are designed to operate at 120K. The large area detector arrays are fabricated using our standard focal plane processes incorporating our recent improvements in operability. ROICs were thinned and bonded to thermally compensating shims to give excellent FPA thermal cycle reliability. Both MW and SW staring FPAs were hybridized and tested with excellent results.

Our technical approach for the SWIR and MWIR HgCdTe photodiode array is the backside-illuminated P-n mesa heterostructure configuration. Detector material is grown on CdTe substrates using our standard LPE processes, with a horizontal slider used to grow the IR absorbing base layer, and a vertical slider used to grow the junction-forming cap layer. Mesa photodiodes are formed by straightforward damage-free wet etching. The passivation is the standard Lockheed Martin CdTe process, which has been shown to be able to make detectors hard to total dose levels in excess of 1Mrad(Si). A multilayer broadband antireflection coating is applied to the CdZnTe entrance surface to reduce reflection losses to less than 1% over the specified wavelength bands while giving high detector quantum efficiency.

The EDR FPA signal chain is designed for high performance at low and high backgrounds. The input cell uses the Charge Transimpedance Integrating Amplifier (CTIA) approach, with two integration capacitors selectable by an MOS switch for optimization of gain. The input cell has an anti-blooming feature that maintains detector bias even after the ROIC input saturates. The CTIA input is followed by two sample and hold capacitors, one for high gain and one for low gain. The gain is set by the integration time prior to the two sample and holds. This integration time is adjustable as is the ratio between the two integration times. The nominal long integration time (high transimpedance gain) is 18 ms and the nominal gain ratio is 64. The automatic gain circuitry compares the outputs with two gains and selects the higher transimpedance gain signal to be read out unless it is saturated. If it is saturated in high gain, then the low gain signal is selected. The gain selection is latched as digital data and read out through parallel digital outputs from the FPA. The analog signal is multiplexed and read out from the ROIC through a differential output. A slew-enhanced output buffer drives a large 100pF output line capacitive load with short settling time. On-chip bias generators compensate for threshold shifts due to temperature or radiation. All the clock signals necessary to operate the FPA are generated from four input clocks.

The FPA design is based on thinning the silicon ROIC to 5 mils thick and gluing it to a supporting shim. The structure is designed such that the resulting thermal expansion characteristics of the Si surface closely approach those of CdTe. This structure has been shown through both analysis and test to be capable of surviving over 200 thermal cycles from room temperature to 80K without degradation in detector/ROIC interconnect. Electrical connection to the FPA is made by wire bonding the ROIC to pads to an intermediate patterned alumina bonding strip mounted on the supporting shim adjacent to the ROIC. Then bonding to the FPA is made from the pads on the alumina board, so multiple rebonds are possible if necessary.

2.0 DETECTOR PERFORMANCE

Detector performance was evaluated using test chips on each wafer. The test chip contained mini-arrays with the same device configuration as the staring and scanning arrays, as well as other diagnostic devices. Test chips were hybridized to fanout boards and tested in metal dewars. Data shown below are for mini-arrays in the staring configuration.

Thanks to multilayer antireflection coatings and good internal collection efficiency, the detectors had excellent quantum efficiency. Figures 1 and 2 show plots of normalized quantum efficiency and back-surface

reflectance for detectors in the SW and MW bands, respectively. Reflectance losses were particularly low, less than 1.5% in the bands of interest. Absolute quantum efficiencies were over 90% for both SW and MW detectors.

Detector I-V curves were well-behaved with very low leakage currents. Zero-bias and reverse bias impedances of the SW devices were too high to measure at 120 and 140 K (over $5x10^{10}$ ohm). MW detectors, however, could be measured. I-V curves of a typical MW detector at three temperatures are shown in Figure 3. The devices are completely diffusion current limited at 140 and 160 K for forward and reverse bias. At 120 K there is a small additional current mechanism at large reverse bias, but the I-V curve is diffusion limited at the operating voltage. RoA followed a diffusion current temperature dependence over the 120 to 160 K range, as seen in Figure 4. Detector noise was white and agreed with the expected value based on Johnson and shot noise. 1/f noise was too low to measure, with a corner frequency less than 1 Hz. The SW and MW detectors met the spatial crosstalk requirements of < 5 percent of the illuminated pixel signal for adjacent detectors with a measured crosstalk to the center of the adjacent pixel of 1.9%.
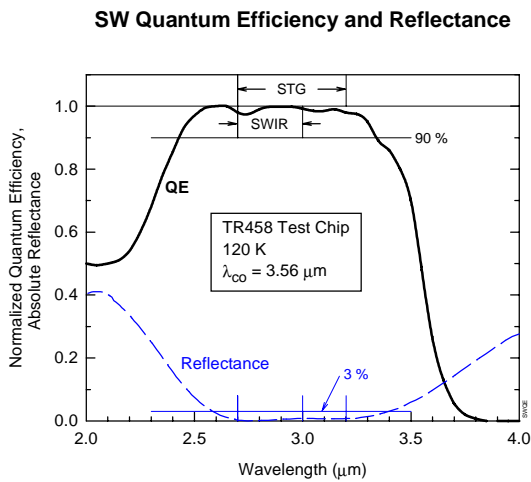

Figure 1.   **Normalized quantum efficiency at 120 K for an SW detector. Reflectance was measured at room temperature on a witness sample from the antireflection coating deposition.**
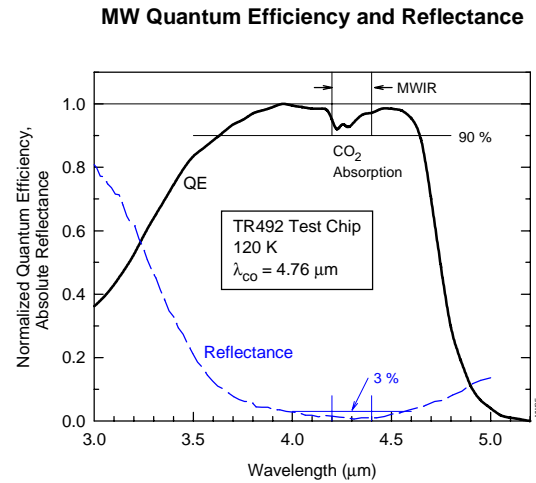
Figure 2.   **Normalized quantum efficiency at 120 K for an MW detector. The dip in QE is an artifact of residual CO_2 absorption in the FTIR spectrometer.**

Current-Voltage Characteristics
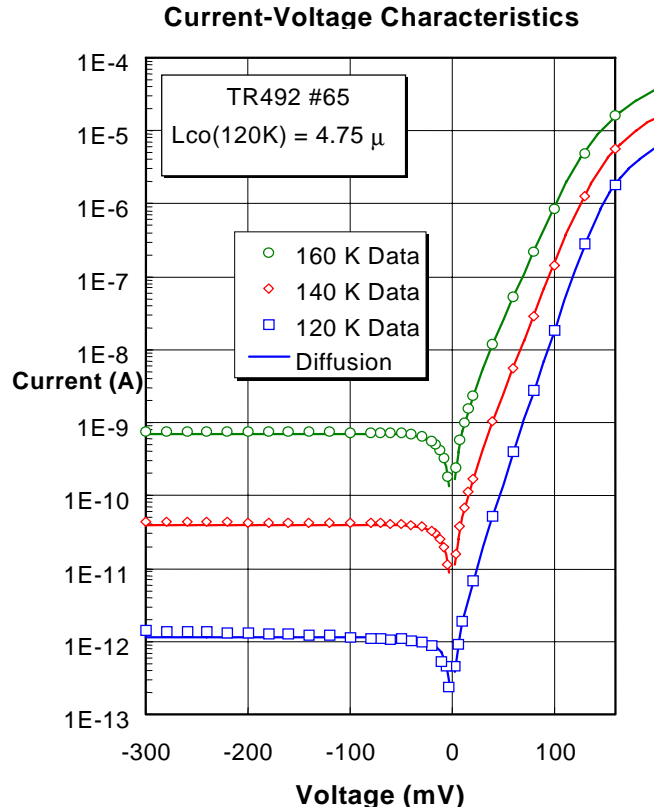
Temperature Dependence of RoA

Figure 3. Current-voltage curves for an MW
detector at three temperatures. The
solid lines fit the data with the voltage
dependence of the diffusion current
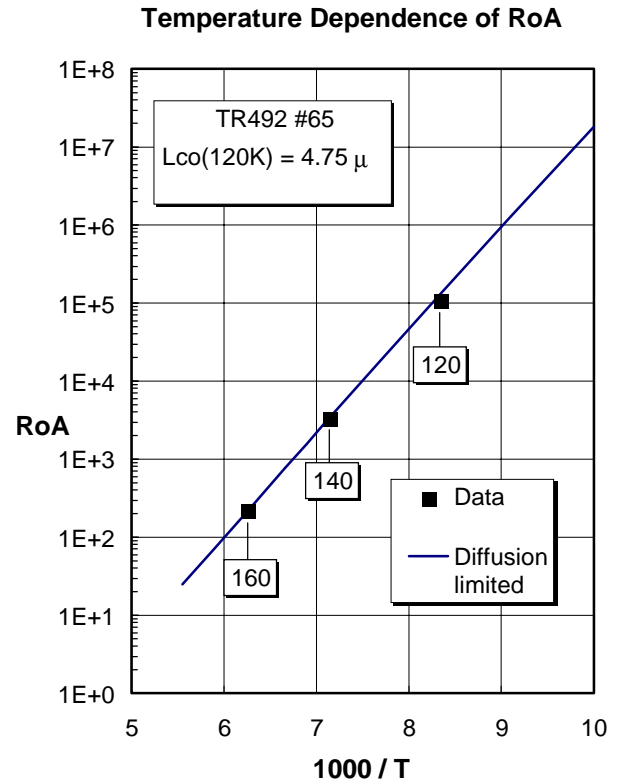mechanism. The fit also includes
series resistance.

Figure 4. Temperature dependence of RoA
for an MW detector.

3.0 ROIC PERFORMANCE

The ROIC met its design goals. The ROIC had a voltage range over 2.5V, with output settling less
than 300ns into a 100pF load. Input bias variation is excellent with only 12mV peak to peak and a standard
deviation of 2.6 mV. This variation was measured on single columns of the ROIC using the test input
circuitry to directly read out the input bias from the selected pixel.   This good threshold uniformity is typical
of what we see from the LMFS foundry. The on-chip detector common generator gives a nominal bias that is
right on target at 17 mV. Therefore the detectors on the FPA will see biases from 11 mV to 23 mV. Only in
1 FPA did we see a benefit in changing the bias from its nominal value. For all of our FPA testing, the
internal detector common generator was used. This on-chip detector common bias generator is critical for
maintaining radiation hardness, compensating for temperature shifts and rejecting power supply noise. The
necessity of an on-chip detector common generator is due to the single-ended CTIA input amplifiers, as
opposed to differential CTIA input amplifiers. A single-ended amplifier has lower power, lower noise and
takes much less layout area than a differential input. However, its input bias voltage is set by a FET

threshold in each input amplifier. With radiation or temperature changes, this threshold changes which will change the detector bias unless the detector common tracks the input amplifier bias. Our on-chip detector common generator does track the bias with a replica CTIA input amplifier eliminating temperature and radiation effects as well as supplying power supply rejection.

The ROIC readout noise of 180 μVrms, which includes all kTC noises, meets the design goal of under 300 μVrms. This results in an excellent low flux NEI for the FPA. The FPAs met the 90 mW power specification at the 10 Hz rate, with measured power on 4 FPAs ranging from 73 to 84 mW. The measurements were taken with a 17.4 Hz frame rate with input amplifiers powered continuously.

4.0 FPA RADIOMETRIC PERFORMANCE

The FPAs demonstrate near BLIP NEI for both SW and MW bands with good operability and uniformity. Response nonlinearity is low, typically 0.5%. The output level is uniform, meeting the 12% of range specification. Spatial crosstalk is less than 3% to the adjacent pixel, even after the ROIC has reached 3 times the saturation level. Temporal crosstalk (frame to frame) is less than our measurement limit of 0.5%. NEI, as well as response and output level, were measured at 120K with an integration time of 18ms for high gain and 281 μs for low gain. A 3.0 μm spike filter was used for the SW measurements. For the MW NEI measurements, a 4.0 μm spike filter was used. Our new 3 MHz 16 bit SDAS data acquisition system was used. Noise was measured with 100 samples. All FPA testing was done at a 1.4MHz pixel rate driving a 120 pF load. NEI has also been measured for FPA1 with a 2.4 MHz pixel rate. Under this condition the output settled in less than 300 ns and the NEI was the same as reported above for FPA1. The minimum flux FPA output noise was also the same with the fast settling, 180 μVrms.

NEI

The LMIRIS staring FPAs demonstrated excellent NEI for both SW and MW FPAs. Two examples of the excellent NEI achieved by our SW and MW 432×432 Staring FPAs at T=120 K are shown in Figures 5 and 6. The SW histogram is for FPA 7, which had a 99.1 % NEI operability. The SW NEI data were taken at slightly above the nominal background irradiance, where the BLIP NEI is 2.4×10^9 ph/cm^2-s. The MW histogram is for FPA 15, which had a 97.2 % NEI operability. The MW NEI data were taken at the nominal MW background irradiance, where the BLIP NEI is 5.9×10^9 ph/cm^2-s.
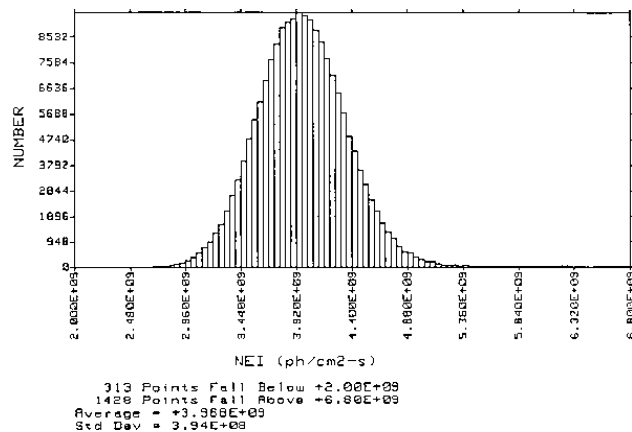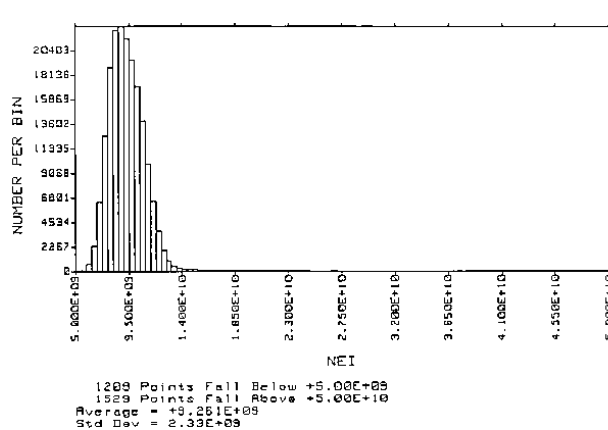

Figure 5. SW FPA 7 NEI at 120K   **Figure 6. MW FPA 15 NEI at 120K**

Table 1. Staring NEI Summary

FPA#	Band	Median NEI (ph/cm^2-s) @Background Level			NEI Operability
		Low	Intermediate	Nominal	Nominal Bkg.
1	SW	1.5E9	2.5E9	3.1E9	98.0%
7	SW	1.5E9	2.4E9	3.0E9	99.1%
6	SW			3.9E9	97.9%
15	MW	5.7E9	6.4E9	8.6E9	97.2%
		Background Photon Flux for NEI Measurements (ph/cm^2-s)			
		Low	Intermediate	Nominal	
Flux	SW	1E11	9.0E11	1.8E12	
Flux	MW	2.4E11	2.0E12	8.1E12	

Both SW and MW FPAs have good NEI performance with excellent operability of 97% to 99%, as can be seen in Table 1. The readout noise limited NEI is seen for the SW FPAs at the low background, 1.5E9 ph/cm^2-s.

Responsivity

Excellent responsivity data was measured on the staring FPAs. The average response values correspond to quantum efficiencies of better than 80%. The operability was excellent as were most of the response nonuniformities. A summary of the data is shown in Table 2. Operability is taken against a 1:1.35 ratio window for response in both high and low gain. SW FPAs show excellent response uniformity. The 1:1.35 response window converts to an effective standard deviation of 5%. FPA 1 has a responsivity standard deviation over the mean of 2.4% and FPA 7 had 2.8%. A histogram of SW FPA 7 high gain response is shown in Figure 7 and SW FPA 15 high gain response in Figure 8.

Table 2. Staring Responsivity

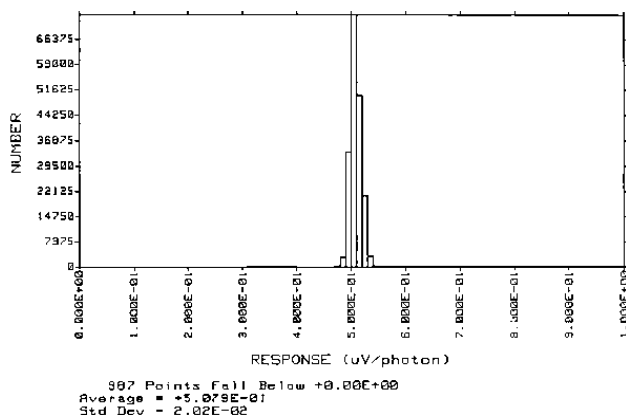| FPA #	Typical High Gain Response (µV/ph)	High Gain Op.	Typical Low Gain Response (µV/ph)	Low Gain Op.
1	0.69	98.1%	0.61	97.6%
7	0.68	99.1%	0.64	99.2%
6	0.69	98.3%		
15	0.44	98.4%	0.42%	96.4%

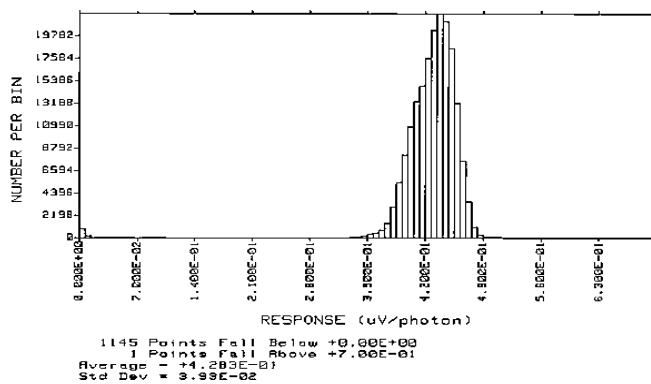**Figure 7. Histogram of FPA 7 High Gain Response   Figure 8. Histogram of FPA 15 High Gain Response**

Output Level Uniformity

Output operability of all the FPAs was good, ranging from 98-99%. The variation in output as a fraction of the range is quite low. A 12% specification translates to a standard deviation over the range of about 2%. For FPA 1 the measured value is 1.3%, for FPA 7 this is 0.9%, and for FPA 13 this is 2.0%. The useful output range of the FPA is 2.2V. The window for the output level uniformity is specified at 12% of the range, which is 0.26V. A histogram of FPA7 output level is shown in Figure 9.
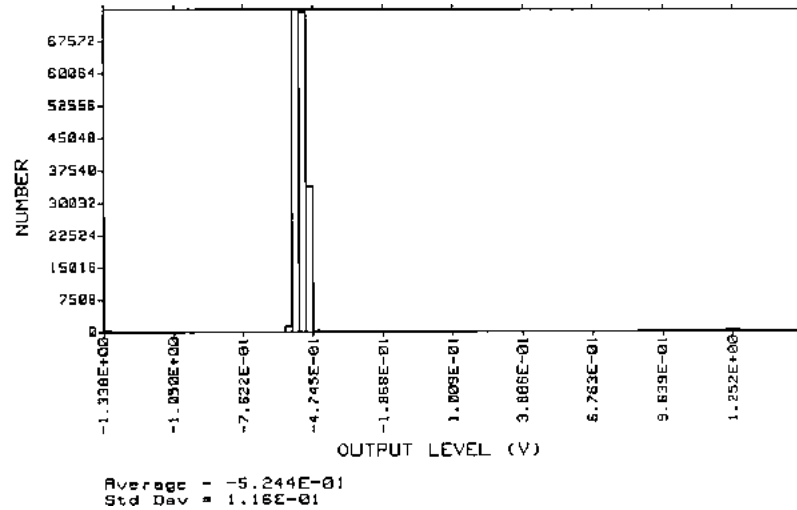

Average = -5.244E-01
Std Dev = 1.16E-01

Figure 9 Histogram of SW SCA7 Output Level

Dynamic Range

The FPA dynamic range is exceptionally high due to the ROIC autogain capability. The maximum instantaneous dynamic range is given by:

IDR= Autogain ratio * Voltage range / FPA noise floor

For the SW FPAs, the autogain ratio of integration times is 64, the voltage range is 2.2V and the minimum FPA noise is 180 µVrms (SW). This gives an instantaneous dynamic range of 780,000 or 118dB for this FPA. The MW range is about half that since the minimum noise is limited by the detector Johnson noise rather than the ROIC.

The maximum high gain flux of the FPA in SW mode is 1.2E13 ph/cm^2-s. The maximum high gain flux in the MW integration mode is 50% higher due to the larger charge capacity. In this mode, the maximum high gain flux is 1.8E13 ph/cm^2-s. However, all the FPA data presented was taken in the SW mode.

Spatial Crosstalk

The total FPA crosstalk is measured to be less than 3%. The ROIC crosstalk to adjacent pixels is less than 1%, and is not measurable beyond adjacent pixels. Not measurable corresponds to less than 0.2%. The detector crosstalk to adjacent pixels is 1.9%. The FPA crosstalk is the combination of the two crosstalks which is less than 3%. Crosstalk beyond adjacent pixels is not measurable.

Blooming is an excessive crosstalk at very high fluxes. While the traditional type of blooming cannot occur in our CMOS readout, there is an issue of increased crosstalk to neighbors due to loss of bias control of detectors after the ROIC input saturates. Anti-blooming circuitry in the input circuit maintains bias even after the integration capacitor is saturated, whether in high gain or low gain. This circuitry should maintain bias up to an input flux of 1.4E16 ph/cm^2-s. Comparison of measurements of the crosstalk below ROIC saturation with crosstalk at 3 times the low gain ROIC saturation confirmed that the crosstalk was unchanged after ROIC saturation.

Thermal Cycling Stability

Temperature cycling tests for the 432x432 FPA were accomplished. The temperature cycling range for these tests were from 80K to 300K. FPA #005, selected for these tests, showed no pixel interconnect deterioration or performance degradation for the 200 cycles tested. The interconnect did not degrade below the excellent 99.98% level measured after the first cooldown, corresponding to about 40 opens out of the 186,624 pixels in the FPA. These tests convincingly demonstrate that our FPA structure exceeds all thermal stability requirements and that it is very robust under thermal cycling.

5.0   SCANNING EXTENDED DYNAMIC RANGE FPA

The extended dynamic range concept has also been successfully implemented in a 768 x 6 TDI scanning FPA. Both SW and MW Hg CdTe photodiode arrays are compatible with a single scanning ROIC design. The detector input stage uses a Charge Transimpedance Integrating Amplifier (CTIA) for superior linearity, and augmented with an anti-blooming circuit. To achieve the high transimpedance gains necessary with these low backgrounds the integration capacitor is only 10 fFd. Double correlated sampling is used to eliminate the noise due to the reset of the integration capacitor.   The Time-Delay-and-Integration, TDI, is performed in a unidirectional tapered CMOS bucket brigade shift register with bi-directional scanning handled by switches to properly address the TDI input cells. Excellent charge transfer, better than .9998, is achieved with our approach using standard CMOS processing. The TDI outputs are multiplexed, converted to voltage and buffered by a linear output stage. Bad pixel deselection is provided to eliminate those rare bad elements that impair the performance of a TDI signal channel.

To achieve the high dynamic range a novel dual gain approach is employed that does not require additional detectors rows.   Every line is evaluated with both a short and long integration interval. If the high gain, long integration time signal saturates the low gain short integration signal is substituted.

Typical noise equivalent input performance is shown in Figure 10 as a function of flux for three different sampling times. The sampling times are 266 µs for the point, 360 µs for the top curve, and 940 µs for the lower curve. This data represent the array average for a SW focal plane operating at 120 K. At very low flux levels the noise is dominated by the read noise of the ROIC and as the flux increases the photon shot noise dominates. The detector noise is very low, in fact, at 145 K the same sensitivity is measured.   Other performance parameters for the scanning focal plane are shown in Table 3.

Table 3. Scanning Focal Plane Performance

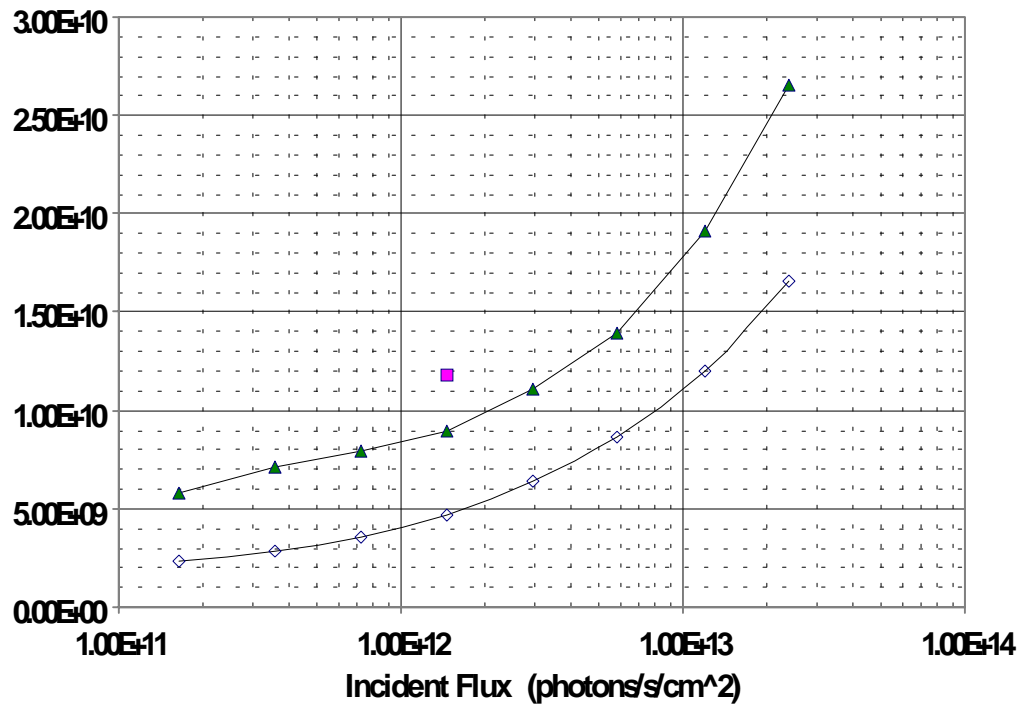| Measurement	Measured Value
Output voltage	>2.5 V
Output Settling time with 100 pF load	<400 ns
Power Dissipation	95 mW
Charge Transfer eff of TDI	>.9998
Readout Noise	180 µVrms
Blooming control	4 voltage levels
Detector bias control	6 biases from 0 to 80 mV

NEI of SWIR Scanning ROIC

Figure 10 Scanning SCA NEI as a Function of Flux and Sample Time

6.0 SUMMARY

LMIRIS has demonstrated 432 x 432 MW HgCdTe Focal Plane Arrays (FPAs) with extended dynamic range. This extended dynamic range concept has also been implemented with 768 x 6 scanning FPAs. These large format staring FPAs are designed for space surveillance applications. The detectors were fabricated using our production LPE material growth process and a multi-layer anti-reflection coating to give high and uniform quantum efficiency of 90% over the large active areas. The ROICs have a dual-gain feature that gives a very high maximum instantaneous dynamic range of up to 118dB. Excellent NEI operability of 99.1% and response uniformity of 2% has been measured. Near BLIP NEI of $3.1x10^9$ ph/cm^2-s has been demonstrated for SW detectors operating at 120K at 1.8E12 ph/cm^2-s background irradiance. An NEI of 8.1E9 ph/cm^2-s has been

measured for MW detectors operating at 120K at 8.0E12 ph/cm^2-s background irradiance. Differential response linearity is typically 0.5%. The FPA is low power, drawing only 85 mW, even though it has a CTIA amplifier input for each detector to give good performance at low backgrounds. These FPAs are designed for total dose hardness and utilize the Lockheed Martin Federal Systems (LMFS) 0.8 μm radiation-hardened CMOS process with two layer polysilicon and depletion mode capacitor options for total dose radiation hardness.

ACKNOWLEDGMENTS

REFERENCES

1. P.H. Zimmermann, D. Baldwin, A. Hairston, J. Wey, P. McDonald, L. Terzis, S. Libonate, J. Czapski, R. Edwards, S. Iwasa, B. Yeadon, et.al. "Scanning and Staring HgCdTe FPA Technology for Space Surveillance Applications," Proc. 1996 IRIS Detector Specialty Group Meeting